

Seasonal Nitrogen Cycles on Pluto

Candice J. Hansen
Jet Propulsion Laboratory
California Institute of Technology
Pasadena, CA 91109 818/354-7675

David A. Paige
Department of Earth and Space Sciences
University of California, Los Angeles
Los Angeles, CA 90024 310/825-4268

March 14, 1994

Submitted to Icarus March 15, 1994

Suggested running title: Pluto's Nitrogen Cycle

ABSTRACT

A thermal model, developed to predict seasonal nitrogen cycles on Triton, has been modified and applied to Pluto. The model is used to calculate the partitioning of nitrogen between surface frost deposits and the atmosphere, as a function of time for various sets of input parameters. Pluto's high obliquity is found to have a significant **effect** on the distribution of frost on its surface. Conditions that would lead to permanent polar caps on Triton are found to lead to permanent **zonal** frost bands on Pluto. In some instances, frost sublimates from a seasonal cap outwards, resulting in a "**polar bald spot**". Dark frost does not satisfy observable on Pluto, in contrast to our findings for Triton. Bright frost comes closer to matching observable, but is not completely satisfactory. Atmospheric pressure variations exist seasonally, but the amplitudes, and to a lesser extent the phase, of the variations depends significantly on frost and substrate properties. In most cases two peaks in atmospheric pressure are observed annually: a greater one associated with the sublimation of the north polar cap just as Pluto recedes from perihelion, and a lesser one associated with the sublimation of the south polar cap as Pluto approaches perihelion. Atmospheric pressure is thus determined both by **Pluto's** distance from the sun and by the subsolar latitude. Our model predicts frost-free substrate surface temperatures in the 50 to 60 K range, while frost temperatures typically fall between 30 to 40 K.

et al, 1993) . If this is the case, Pluto may join Mars and Triton in possessing a climate controlled by a polar-cap-buffered **surface-atmosphere** system. On Mars, and probably on **Triton**, atmospheric pressure varies seasonally as polar caps sublime and condense (Leighton and Murray, 1966, Trafton, 1984, Spencer, 1990). Frost deposit locations and rates of sublimation and condensation are determined by energy balance in the frost deposit, as frost deposit temperature changes and the latent heat of the solid-vapor transition balance incoming solar insolation, emitted thermal radiation, and thermal conduction of heat to and from the subsurface.

On a body whose atmospheric pressure is determined by vapor pressure equilibrium with surface frosts, volatile conditions as a function of time dominate the climate. Forecasting climate forward or backward in time is impossible without incorporation of volatile processes and the physical properties of the frost itself. Frost properties under the cryogenic conditions of the outer solar system are not well constrained however. Frost inventory, emissivity, and **albedo** can take on a large range of possible values. By **modelling** volatile behavior as these parameters are varied, and comparing the model results with observations, we may be able to constrain these frost properties.

We may compare model predictions to observable on both Triton and Pluto. Both Triton and Pluto have a volatile inventory which includes N₂, CH₄, and CO (**Cruikshank** et al, 1984, Cruikshank et al, 1991, Cruikshank et al, 1993, Owen et al, 1992). Both have thin atmospheres dominated by nitrogen (Broadfoot et al, 1989, Tyler et al, 1989, Elliot et al, 1989, Hubbard et al, 1989, Owen et al, 1993) . Both exhibit bright south poles, from which one might expect frost to have sublimated (Stansberry et al, 1990, Hansen and Paige, 1992), as both bodies have experienced sunshine at southern latitudes during this epoch. The two bodies have similar size, density, rotational periods, and, when Pluto is at perihelion, their distance from the sun is comparable. They may have had a similar origin early in the history of the solar system (Stern, 1991) .

Impressive data sets have been acquired for Pluto by **earth-based** observers. Disk-integrated brightness and rotational light curves have been measured. Observations of the secular decrease in Pluto's brightness and accentuation of its rotational light curve since 1955 are summarized in Stern et al, 1988. The recent series of Pluto-Charon mutual events have yielded **albedo** maps of Pluto's surface (Young and **Binzel**, 1993, Buie et al, 1992). These maps show a bright south polar region, a dark mid-southern latitude region, a bright mid-northern latitude region, and a dark region at higher northern latitudes. A fortuitous stellar occultation in 1988 allowed the measurement of Pluto's atmospheric pressure. Assuming that nitrogen is the dominant constituent, the pressure is on the order of 0.1 to 0.5 Pa (Elliot et al, 1989, Hubbard et al, 1989) . **Pluto's** disk-integrated brightness temperature has been measured both at far IR (Sykes, 1993) and at millimeter wavelengths

(Weintraub et al, 1993) but the two data sets don't seem to agree unless a wavelength dependent emissivity is invoked (Sykes, 1993). The challenge now is to pull all these observations together into a general picture of what may be taking place on Pluto. To do this one must disentangle temporal variability due to changes in the observing geometry of Pluto from the earth, from temporal changes due to volatile transport. One approach to this is to apply a thermal model to **Pluto's** seasonal nitrogen cycle.

There are two valuable results which come from **modelling** a problem. First is the capability to analyze trends as parameters are varied. This trend analysis can be used in our application to constrain frost properties. The second important capability is to pin down a set or set of parameters consistent with Pluto observations, and then proceed to address specific questions relevant to understanding what may really be taking place on Pluto.

The Pluto questions which we wish to address with our model are as follows:

1. Can Pluto observations be described in terms of a N₂ atmosphere in vapor pressure equilibrium with surface frost deposits?
2. How does Pluto's eccentric orbit and high obliquity affect its volatile distribution?
3. What surface and frost temperatures are likely, as a function of time, for a body at **Pluto's** distance from the sun?
4. Can we bound a range of possible atmospheric pressure levels and variation for planning purposes for Pluto mission opportunities?
5. What insights gleaned from modeling volatile behavior on Pluto are applicable to Triton? As input parameters are varied, do we note the same trends in volatile partitioning and distribution as previously determined for Triton (Hansen and Paige, 1992)? Can a comparison of Pluto and Triton shed light on the Triton bright frost / dark frost enigma (Spencer, 1990, Stansberry et al, 1990, Hansen and Paige, 1992, **Eluszkewicz**, 1991, **Duxbury** and Brown, 1993)?

The model we have used is a direct adaptation of our Triton thermal model, modified to apply to Pluto. Hansen and Paige (1992) originally modified a Mars thermal model to apply to conditions on Triton. This thermal model is based on the successful Leighton and Murray (1966) diurnal and seasonal formulation of the heat balance of the polar caps on Mars. The model solves the frost energy balance equation to calculate sublimation and condensation rates as a function of time and latitude. The primary input parameters are the **albedo** and emissivity of the frost, the **albedo** and thermal inertia of the substrate, and the total nitrogen inventory. The model outputs frost deposit locations as a function of time, which

can be compared to **albedo** boundaries observed on Pluto, and atmospheric pressure and disk-integrated brightness and temperature, which can be directly compared to earth-based measurements of these quantities on Pluto.

The Pluto Thermal Model

The thermal model used for Pluto is a direct adaptation of the Triton thermal model described in detail by Hansen and Paige (1992). Briefly, the Pluto thermal model solves the heat balance equation shown in Figure 1 four times per Pluto hour at 18 latitudes. Frost is sublimed or condensed locally at a rate consistent with maintaining global vapor pressure equilibrium, and conservation of mass and energy. The model transitions from a state in which an atmosphere exists and frost temperature changes are controlled by vapor pressure equilibrium, to an atmosphereless state in which little or no latent heat is available, and frost temperature changes are dominated by radiative balance.

Table 1 lists some of the most important variables in the model and shows again the considerable degree of similarity between Triton and Pluto. It was not necessary for example, to change the interior heat flux, which was set to 6 mW/m^2 for Triton - the similar densities of the two bodies would lead one to predict similar rock content (Null et al, 1993, Brown et al, 1991). Likewise, the rotational periods are close enough that the depth of the diurnal thermal wave is similar, thus the algorithm used to determine the thicknesses and the number of layers in the substrate could be left unchanged. The top three layers are set to 1/4 the depth of the diurnal thermal wave, with subsequent layers thickening by a factor of 1.13, and we are **using** 60 layers.

The frost deposit is assumed to be isothermal, which is equivalent to assuming that the frost is porous enough to remain in vapor pressure equilibrium with the atmosphere. The model makes predictions based on pure nitrogen frost. Recent spectral data would indicate that this should give realistic results because nitrogen is by far the dominant volatile constituent, with CO and CH₄ present only in trace amounts (Owen et al, 1993).

The Pluto thermal model tracks whether nitrogen is in its alpha or beta state. This is a significant change from the Triton model. Solid nitrogen undergoes a phase transition at a temperature of 35.61 K from a hexagonal crystal structure ($T > 35.61 \text{ K}$) to a cubic structure ($T < 35.61 \text{ K}$). The model now stops its normal routine when the transition temperature is reached and devotes all energy to the latent heat of the alpha-beta transition, $8.18 \times 10^3 \text{ J/kg}$ (Johnson, 1960). Frost temperature remains constant and no frost is allowed to sublime or condense until the transition from alpha to beta or beta to alpha is complete. The model tracks whether frost is in its alpha or beta state at all times. The

latent heat of the solid-vapor transition is the appropriate value for the phase of the solid: $2.5e5$ J/kg for beta frost, and $4.3e5$ J/kg for alpha frost (Brown and Ziegler, 1980) .

Pluto's orbit and obliquity enter into the solar insolation term in the heat balance equation. **Pluto's** orbit is the least circular of all the planets in the solar system, with an eccentricity of 0.249. Its obliquity is high, 119.998 deg (derived from Null et al, 1993). Planets that have **obliquities** greater than approximately 54 degrees, have annual insolation at the poles that is greater than the annual insolation at the equator (Ward, 1974) . Currently **Pluto's** orbit orientation is such that the sun crosses Plutoss equator at perihelion and aphelion. One might expect that this would affect seasonal frost deposition patterns, as illustrated in Figure 2, and this expectation is borne out by model results.

MODEL RUNS

Over 25 different cases have been run for Pluto. See Table 2. The primary input parameters varied between runs are: substrate **albedo** and thermal inertia, frost **albedo** and emissivity, and total nitrogen inventory. All properties remain constant with time and no hemispheric differences have been assigned in runs to-date.

On Pluto, as determined from the series of mutual events, surface **albedo** varies from a low of 0.15 to a high of 0.9 (Buie et al, 1992, Young and Binzel, 1993). Most of the model runs assigned an **albedo** of 0.2 to frost-free substrate and 0.8 to the frost, or 0.8 to the substrate and 0.2 to the frost. As on Triton we wanted to test a "**dark frost**" hypothesis, although it is harder to imagine a dark frost with an **albedo** of 0.2, than it was to imagine a frost on Triton that was just relatively dark, with an **albedo** of 0.6.

Substrate thermal inertia was assigned values of 1, 7, or 50×10^3 **cal/cm²-K^{-sec}^{1/2}**. A thermal inertia of 1 is similar to that derived for Rhea (Spencer and Moore, 1992), and estimated for surfaces of fine-grained icy satellites (Morrison and Cruikshank, 1973) ; a thermal inertia of 50 is appropriate for solid water ice. Table 3 gives the depth of the diurnal and seasonal thermal waves for each of these three values.

Frost emissivity was varied from 0.6 to 1.0. Atmospheric pressure is a strong function of frost emissivity (Nelson et al, 1992), and thus the range of emissivity values **modelled** could be constrained by observed atmospheric pressure. The globally averaged **nitrogen** inventory was set at either 50, 100, or 200 **kg/m²**. This very important parameter is poorly constrained (Cruikshank et al, 1984, Duxbury and Brown, 1993).

MODEL RESULTS

Model output is shown in the figures that follow. **All** data is plotted as a function of time from 1000 to 2100 AD. The top panel gives Plutots distance from the sun in AU for reference. Pluto's highly eccentric orbit is obvious. The second panel plots whole disk **albedo**. This is simply a sum of surface area with and without frost, weighted as Pluto would have been viewed from the earth.

The third panel gives temperatures. Figure 4 and subsequent figures "plot four temperatures. (Figure 3 **has** a different convention than subsequent figures and use of this panel is described in the caption.) The solid line is the frost temperature. This has a direct correspondence with atmospheric pressure due to the constraint of maintaining vapor pressure equilibrium. The fine-dotted line is the warmest surface temperature of the substrate, anywhere on the planet, at the given time. The dot-dash line gives the disk-integrated brightness temperature at a wavelength of 60 microns. The dashed line gives the disk-integrated brightness temperature at 1300 microns. These two temperatures are determined by calculating the emitted flux for each element visible from the earth, based on its temperature and emissivity.

The fourth panel shows atmospheric pressure as a function of time in **pascals** on a log scale. The bottom panel shows at which latitudes frost deposits occur as a function of time. The stippled area is the area predicted to be covered by frost. The sawtooth curve plotted in this panel is the **subsolar** latitude. It is a sawtooth curve because of Pluto's eccentricity: the sun crosses from -60 to +60 deg latitude quickly as Pluto moves through perihelion, but crosses from +60 to -60 slowly as Pluto moves through aphelion.

Trends

THERMAL INERTIA

High Thermal Inertia:

All bright frost runs with a high thermal inertia substrate formed permanent **zonal** bands rather than polar caps. See Figure 3. This was clearly the result of Pluto's high obliquity. On a seasonal time scale, higher thermal inertia surfaces required longer to cool off or to warm up, thus remained closer to their annual average temperatures. As noted, Plutots annual average insolation is higher at its poles than at its equator because of its obliquity. The exact latitude zone at which the band formed was not significant - it depended on the Pluto season at which the run was initiated. (This was determined by initiation of several runs at different times during the Pluto year). The **zonal** bands were permanent because the high thermal inertia substrate warmed up

and then stayed warm at the poles, due to the higher insolation, preventing the condensation of new frost. The **albedo** difference between a dark, heat-absorbing substrate and a bright reflective frost further reinforced the stability of the **zonal** band. Frost temperature was very stable, remaining very close to 35 K in this particular run, thus flattening out seasonal variations in atmospheric pressure. The surface temperature of frost-free substrate reached 50 K when the subsolar point reached its most extreme latitude.

Moderate Thermal Inertia:

Moderate thermal inertia runs with a low nitrogen inventory predicted seasonal polar caps. In many cases these seasonal caps sublimated from the pole out, developing a "**polar bald spot**". See Figure 4. The polar caps were asymmetric: the south polar cap persisted through the slow excursion through aphelion, while the short-lived north polar cap was in place during perihelion.

Substrate temperatures were calculated to reach 55 K, while the frost temperature stayed between roughly 34 and 40 K. High temperatures were correlated with extreme subsolar latitude. The disk-integrated brightness temperature predicted at 1300 microns is observed to dip below the frost temperature - this was **due to** the frost emissivity, which for this run was set to 0.6. If this were the real Pluto, an earth-based observer in 1982 would measure a brightness temperature at 60 microns of approximately 48 K, while in 1991 an earth-based observer would measure a temperature at 1300 microns of approximately 38 K. Assignment of an even **lower** emissivity to the frost would further widen this apparent temperature difference.

Some cases were transitional in nature, with a permanent **zonal** band and seasonal polar caps. This generally happened for moderate inertia cases when the frost was cold, as is the case for a high emissivity or high **albedo** frost. High inventories of nitrogen also led to this configuration, as shown in Figure 5, which was a low thermal inertia case. Some frost was mobile enough to move around seasonally and form polar caps, but the rest remained in the stable **zonal** band.

Low Thermal Inertia:

Low thermal inertia cases with low nitrogen inventories, and all dark frost runs, formed seasonal polar caps. These caps condensed earlier and sublimated earlier than moderate inertia cases. See Figure 6. Seasonal variation in atmospheric pressure was most pronounced for low thermal inertia runs. Two pressure peaks per Pluto year were predicted. The two atmospheric pressure minima were directly correlated to the condensation of the northern and southern caps. The pressure peak associated with the sublimation of the southern cap as Pluto approached perihelion was typically

lower than that associated with the sublimation of the northern cap as Pluto receded from perihelion.

The highest surface temperature of frost-free substrate was predicted to reach 60 K. The frost temperature in this run varied from 26 to 36 K. The emissivity for this run was set to 0.8, but the brightness temperature detected at 1300 microns never dipped below the frost temperature because there was always a substantial expanse of warm substrate in view, as compared to the case illustrated in Figure 4. Peaks in frost temperature were correlated with the subsolar latitude. Increases and decreases in the other three temperatures tracked increases and decreases in whole disk **albedo**. If this were the real Pluto the brightness temperature measured at 60 microns **in** 1982 would be approximately 53 K. In 1991 the brightness temperature at 1300 microns would be roughly 46 K.

EMISSIVITY

As has been noted by other authors (Stansberry et al, 1990, Nelson et al, 1992), an increase in frost emissivity corresponds to a decrease in atmospheric pressure. High emissivity frosts are colder than low **emissivity** frosts. Emissivity values lower than 0.6 predicted atmospheric pressures far higher than the value measured during the stellar occultation in 1988. Model runs also suggest that high emissivity bright frosts won't condense as far equatorward as low emissivity frosts, and tend to condense later.

N2 INVENTORY

The nitrogen inventory has a significant effect on polar cap deposits, and is one of the most poorly constrained parameters. A large frost deposit will change temperature slowly, because of its significant heat capacity. It will take longer to **go** through the alpha - beta phase transition than a thin deposit, thus delaying subsequent sublimation or condensation. This has in fact been proposed as the mechanism for maintaining a bright nitrogen polar cap on Triton, at a season when it is not expected to be stable (**Duxbury** and Brown, 1993). Figure 5 shows a run with a global nitrogen inventory of 100 **kg/m**2**. The only difference between the runs shown in Figure 5 and Figure 6 is that the **nitrogen** inventory was doubled. This small change caused the model to predict permanent **zonal** bands in addition to seasonal polar caps. As nitrogen was stabilized in the **zonal** band, seasonal variation in atmospheric pressure was flattened out substantially.

Discussion

BRIGHT FROST/DARK FROST ENIGMA

On **Triton**, one of the most intriguing questions raised after the Voyager flyby, was "which is the polar cap - the bright deposit seen in the southern hemisphere or the (relatively) dark northern hemisphere?". Early thermal modelling by Stansberry et al (1990), and later efforts by Hansen and Paige (1992), showed that a bright seasonal nitrogen cap would not be stable in southern summer at the time of the Voyager flyby. Spencer (1990), proposed that the nitrogen frost was relatively dark, and **Eluszkiewicz** (1991) proposed that freshly condensed nitrogen would be transparent. Hansen and Paige found that a relatively dark or transparent frost yielded predictions of observable consistent with Voyager observations. These were not the only possible explanations - other possibilities included: 1) a bright permanent N₂ cap produced and maintained by anisotropic internal heat flow (Brown and Kirk, 1991); 2) a permanent **albedo** difference of the substrate which affects the radiative balance (Moore and Spencer, 1990); 3) N₂ ice shattered by going through the alpha-beta phase transition, and thereby changing its radiative properties (**Eluszkiewicz**, 1991, **Duxbury** and Brown, 1993, Tryka et al, 1993); and 4) a bright lag deposit of less volatile CH₄ and possibly CO and CO₂ ices (Grundy and Fink, 1991, Cruikshank et al, 1991, Trafton, 1992).

On Pluto it is far more difficult to conceive of a process by which frost is formed which is really dark (-0.2 **albedo**), not just relatively dark (0.6 **albedo**). If a darkening process could be imagined, it must also be active only on Pluto and not on Triton. Dark frost runs of our model did not yield predictions at all close to **Pluto's** observable. Figure 7 is a run with the parameters that gave the best fit to Triton observable. This run, as was the case with other dark frost runs, predicted that bare bright substrate would be observable from the earth from 1955 to 1990, but that this bright ground would be visible to far above the equator, thus no dark mid-latitude band in the south was predicted. Atmospheric pressure was too high to match stellar occultation results. No differences between 60 and 1300 micron brightness temperatures were predicted. A dark frost does not rescue us on Pluto as it did on Triton, however a transparent frost cannot be ruled out.

PLUTO'S THERMAL SIGNATURE

IRAS' detection of Pluto at 60, 80, and 100 microns in 1982 led Sykes (1993) to conclude that **Pluto's** surface temperature was in the range of 55 to 73 K. A warm surface could co-exist with up to a projected area of 33% frost with a temperature of 35 K and be consistent with IRAS data (Sykes, *ibid*). This seemed to be at variance with millimeter wave measurements acquired in 1991, which have been interpreted to indicate a surface temperature for Pluto

that is in the range of 30 to 44 K (Weintraub et al, 1993), unless wavelength-dependent emissivity was invoked (Sykes, 1993). Our results show that nitrogen ice will be **"patchy"** on a latitudinal scale (either in **zonal** bands or permanent caps, but not covering the planet globally). We predict frost temperatures between 25 and 40 K, and maximum surface temperatures for unfrosted areas to be in the 50 to 60 K range, depending on substrate thermal inertia. Our model predicts that the temperature measured at the earth depends significantly on the viewing geometry from the earth. Figure 4 for example showed a case in which at **times**, although the surface was much warmer, the viewing geometry was such that the measurement made from the earth would be the temperature of the polar cap frost. **Furthermore** the brightness temperature measured at 60 and at 1300 microns is a function of time, as frost and surface temperatures change and the frost moves around. We can attribute as much as a 10 K difference in the results at 60 and 1300 microns to the combination of temporal changes in surface and frost temperatures and the change in viewing geometry.

MATCH TO OBSERVABLE

As was the case for Triton, the observed **albedo** boundaries are very difficult to match. We do **not** find in any of our runs a bright nitrogen cap that would persist from 1955 through 1990. We do see cases in which an old south polar cap is still in place in 1955, subsequently sublimates, and a new south polar cap has begun to condense by 1980. This situation would potentially yield a bright south pole, and dark south mid-latitudes with a bright northern hemisphere. The low thermal inertia case illustrated in Figure 8 shows an example of this case, but the atmospheric pressure and **albedo** trends are not good matches to data.

A high thermal inertia substrate with just a permanent **zonal** band (no seasonal caps) can be ruled out because predicted **albedo** markings are completely inconsistent with observations. A **"dark frost"** case can be discarded for reasons given above.

The best match so far to Pluto observable is shown in Figure 9. This run has a moderate thermal inertia, an emissivity of 0.8, and a nitrogen inventory of 50 kg/m^2 . This case is flawed in that it does not predict a bright south polar cap in 1985 (the cap does not begin forming until the late 1990s), but it does still have a bright polar cap in 1955, and shows a decrease in disk-integrated **albedo** as seen from the earth between 1955 and 1985. The atmospheric pressure is in the right ballpark. The brightness temperature measured at 60 microns from the earth in 1982 was predicted to be 47 K, while the prediction for 1300 microns in 1991 was 42 K.

Conclusions

Application of the Triton thermal model to Pluto has enabled comparisons of the seasonal nitrogen cycles on these two bodies. Although they may have formed in the same region of the solar system and share many similarities, their climates today depend most significantly on their current orbital characteristics. Trends have been identified as frost and substrate properties have been varied. We have not yet found a uniform set of parameters which could yield good matches to observable for both bodies.

The failure to find a set of parameters which perfectly matches Pluto observable does not necessarily mean that the assumption of vapor pressure equilibrium was flawed. It does indicate that the situation is more complex than can be described by a simple thermal model. Multi-component ices certainly play a role. Time variability of frost properties may be an important factor. Application of a simple model is just the first step in the process of understanding the real Pluto climate, and trends identified will lead to insight into more complex processes that must be incorporated for the model to be viable.

We have shown that **Pluto's** eccentric orbit and high obliquity have a very significant effect on the condensation and sublimation of its polar caps. The eccentricity of Pluto's orbit is the reason that the northern cap condenses slowly as Pluto moves through aphelion, whereas the southern cap condenses quickly as the sun moves to its most northerly latitude just after perihelion. In many cases the southern cap persists longer than the northern cap because of its slow rate of sublimation. **Pluto's** high obliquity is responsible for the prediction of the formation of **zonal** bands in high thermal inertia cases, and polar bald spots in moderate thermal inertia runs.

The discrepancy between temperatures measured at infrared and millimeter wavelengths may not be as large as previously thought. Model results indicate that a difference of up to 10 K could result from the change in time between the two measurements, attributable to the combination of change in viewing geometry and change in frost and substrate temperatures over the intervening 9 years. The warmest substrate surface temperatures we predict are 60 K for a low thermal inertia run and 50 K for a high thermal inertia run. Frost temperatures ranged from 25 to as high as 40 K, depending on frost parameters assumed.

The atmospheric pressure variations are of perhaps the most interest in planning for future Pluto missions. We find that in most cases the high levels of atmospheric pressure that Pluto is currently experiencing will continue to increase until the year 2000, but will start to drop after 2020. The pressure may drop by many orders of magnitude, and the drop to low pressure will persist through Plutoc's slow excursion through aphelion.

Pluto observable supply an additional set of constraints on frost properties on both **Triton** and Pluto, and to-date a satisfactory match to all observable on both bodies has not been found. Bright nitrogen frost is just too volatile to persist through the southern spring and summer. We are left with the same set of **possible** explanations as previously identified for Triton.

Our future work will focus on these possibilities: 1) A large CH₄ deposit, left behind after sublimation of the seasonal N₂ frost, can be invoked to explain light curve observations, but it will ultimately have to be consistent with spectral observations as well; 2) With the addition of the alpha-beta phase to our model, we are in a position to test the explanation proposed by **Duxbury** and Brown (1993), in which a large inventory of nitrogen frost is stabilized by the the alpha-beta transition; 3) **modelling** of transparent frost cases, in which frost is assigned the **albedo** of the underlying substrate (which may be assigned differing values latitudinally), is straightforward.

REFERENCES

- Binzel**, R. P. (1990), Lunar and Planetary Science Conference, **21:87-88**.
- Broadfoot, L., S. Atreya, J. Bertaux, J. **Blamont**, A. **Dessler**, T. Donahue, W. Forrester, D. Hall., F. Herbert, J. **Holberg**, D. Hunten, V. **Krasnopolsky**, S. Linick, J. **Lunine**, J. McConnell, H. Moos, B. Sandel, N. Schneider, D. Shemansky, G. Smith, D. **Strobel**, and R. **Yelle** (1989), "Ultraviolet Spectrometer Observations of Neptune and **Triton**", Science **246:1459-1465**.
- Brown, G. N., and W. T. Ziegler (1980), "Vapor pressure and Heats of Vaporization and Sublimation of Liquids and Solids of Interest in Cryogenics below 1-atm Pressure", Adv. Cryogen. Engng. **25:662-670**.
- Brown, R. H., T. Johnson, J. **Goguen**, G. **Schubert**, and M. Ross (1991), "Triton's Global Heat Budget", Science **251:1465-1467**.
- Brown, R. H. and R. L. Kirk (1991), "Coupling of Internal Heat to Volatile Transport on **Triton**", BAAS **23:1210**.
- Buie, M. W., D. J. **Tholen**, and K. Home (1992) , "Albedo Maps of Pluto and Charon:Initial Mutual Event Results", Icarus **97:211-227**.
- Cruikshank**, D., R. H. Brown, and R. Clark (1984), "Nitrogen on **Triton**", Icarus **58:293-305**.
- Cruikshank**, D. P., T. Owen, T. **Geballe**, B. Schmitt, C. de Bergh, J-P. Maillard, B. Lutz , and R. H. Brown (1991) , "Tentative Detection of CO and CO₂ Ices on **Triton**", BAAS **23:1208**.
- Cruikshank**, D. P., T. L. **Roush**, T. C. Owen, T. R. **Geballe**, C. de Bergh, B. Schmitt, R. H. Brown, M. J. Bartholomew (1993) , "Ices on the Surface of **Triton**", Science **261:742-745**.
- Duxbury**, N. S. and R. H. Brown (1993), "The Phase Composition of **Triton's** Polar Caps", Science **261:748-751**.
- Elliot, J. L., E. W. Dunham, A. S. Bosh, S. M. **Slivan**, Lo A. Young, (1989), " ", Icarus **77:148-170**.
- Eluszkiewicz**, J. (1991), "On the Microphysical State of the Surface of **Triton**", J. Geophys. Res. **96:217-231**.
- Grundy**, W. M. and U. Fink (1991), "A New Spectrum of **Triton** near the Time of the Voyager **Encounter**", Icarus **93:379-385**.
- Hansen, C. J. and D. A. Paige (1992), "A Thermal Model for the Seasonal Nitrogen Cycle on **Triton**", Icarus **99:273-288**.
- Hubbard, W. B., R. V. **Yelle**, J. I. Lunine (1989), " ", Icarus

84:1-14.

Johnson, V., Ed. (1960), "**A Compendium of the Properties of Materials at Low Temperature (Part 1)**", Wadd Technical Report 60-56.

Leighton, R. and B. Murray (1966), "**Behavior of Carbon Dioxide and Other Volatiles on Mars**", Science **153:136-144**.

Moore, J. M., and J. R. Spencer (1990) , "**Koyaanismuuyaw: The Hypothesis of a Perennially Dichotomous Triton**", Geophys. Res. Lett. **17:1757-1760**.

Morrison, D. and D. P. **Cruikshank** (1973), "Thermal Properties of the **Galilean** Satellitestl, Icarus **18:224-236**.

Nelson, R. M., W. D. Smythe, B. D. **Wallis**, L. J. Horn, A. L. Lane, and M. J. Mayo (1990), "Temperature and Thermal **Emissivity** of the Surface of Neptunets Satellite **Triton**", Science **250:429-431**.

Null, G. W., W. M. Owen, Jr., and S. P. Synnott (1993), "**Masses and Densities of Pluto and Charon**", AJ ??.

Owen, T. C., T. **Geballe**, C. de Bergh, L. Young, J. Elliot, D. Cruikshank, T. **Roush**, B. Schmitt, R. H. Brown, J. Green (1992) "Detection of Nitrogen and Carbon Monoxide on the Surface of Pluto", BAAS **24:961**.

Owen, T. C., T. L. **Roush**, D. P. **Cruikshank**, J. L. Elliot, L. A. Young, C. de Bergh, B. Schmitt, T. **R. Geballe**, R. H. Brown, M. J. Bartholomew (1993), "Surface Ices and the Atmospheric Composition of Pluto", Science **261:745-748**.

Paige, D. (1992), "**The Thermal Stability of Near-Surface Ground Ice on Mars**", Nature **356:43-45**.

Spencer, J. (1990) , "Nitrogen Frost Migration on Triton: A Historical **Model**", Geophys. Res. Lett. **17:1769-1772**.

Spencer, J. R. and J. M. Moore (1992), "**The Influence of Thermal Inertia on Temperatures and Frost Stability on Triton**", Icarus:??.

Stansberry, J., J. **Lunine**, and C. Porco (1990) , "**Zonally Averaged Thermal Balance and Stability Models for Nitrogen Polar Caps on Triton**", Geophys. Res. Lett. **17:1773-1776**.

Stern, S. A., L. M. Trafton, G. R. Gladstone (1988), "Why is Pluto Bright? Implications of the **Albedo** and **Lightcurve** Behavior of **Pluto**", Icarus **75:485-498**.

Stern, S. A. (1991), "On the Number of Planets in the Outer Solar System: Evidence of a Substantial Population of 1000-km **Bodies**", Icarus **90:271-281**.

Sykes, M. (1993) , "Implications of Pluto-Charon Radiometry", BAAS **25:1138**.

Trafton, L. M. (1992), "**Methane** Enhancement in **Triton's** South Polar Cap: Interpretation in Terms of CH₄ and N₂ in Solid **Solution**", Neptune and Triton Conference Abstract.

Tryka, K. A., R. H. Brown, V. Anicich, D. P. **Cruikshank**, T. C. Owen (1993), "Spectroscopic Determination of the Phase Composition and Temperature of Nitrogen Ice on **Triton**", Science **261:751-754**.

Tyler, G., D. Sweetnam, J. Anderson, S. **Borutzki**, J. **Campbell**, v. **Eshleman**, D. Gresh, E. **Gurrola**, D. Hinson, N. **Kawashima**, E. **Kursinski**, G. Levy, G. **Lindal**, J. Lyons, E. **Marouf**, p. Rosen, R. Simpson, and G. Wood (1989), "Voyager Radio Science Observations of Neptune and **Triton**", Science **246:1466-1473**.

Ward, W. R. (1974) , "**Climatic** Variations on Mars: 1. Astronomical Theory of **Insolation**" JGR **79:3375-3386**.

Weintraub, D. A., S. A. Stern, M. C. Festou (1993), "**Millimeter-Wave** Measurements of Plutons Thermal Emission: Evidence for a Cold **Surface**", Pluto and Charon Conference abstract, page 72.

Young, E. F. and R. P. **Binzel** (1993), "Comparative Mapping of **Pluto's Sub-Charon** Hemisphere: Three Least Squares Models Based on Mutual Event **Lightcurves**", Icarus ??.

FIGURE CAPTIONS

Figure 1. This figure illustrates the frost heat balance equation solved by the model. A change in frost temperature, $mC \cdot dT/dt$, is determined by the combination of incoming solar energy, $S_0(1-A)$, the emitted thermal energy, $e \cdot \sigma \cdot T^4$, latent heat of frost sublimation or condensation, $L \cdot dm/dt$, and thermal conduction of heat to and from the substrate, $k \cdot dT/dz$. The change in frost temperature is balanced with frost condensed or sublimed in such a way as to insure conservation of energy and global vapor pressure equilibrium.

Figure 2. **Pluto's** eccentric orbit is expected to affect deposition and sublimation rates of its polar caps.

Figure 3. Model output for a high thermal inertia case (run #32) is shown in this figure. This run had a thermal inertia of $50 \times 10^{-3} \text{ cal / cm}^2\text{-sec}^{1/2}\text{-K}$, a substrate **albedo** of 0.2, a frost **albedo** of 0.8, a frost **emissivity** of 1.0 and a global N₂ inventory of 50 kg / m². This case predicts the formation of a permanent **zonal** band of frost. The latitude at which the band is formed is not significant - the latitude is determined by **Pluto's** season at the time a run is started. Atmospheric pressure is very stable as frost is immobilized in the permanent band. Temperatures plotted in the third panel are the frostpoint temperature (solid line), the north and south pole temperatures (dash and dash-dot lines), and the temperature at +10 deg latitude (fine dot). This illustrates why there are no seasonal polar caps - the polar temperature is never low enough for frost to condense. Peaks in the substrate temperature are observed to correspond to maximum excursions of the subsolar point.

Figure 4. This case illustrates what happens when the substrate is assigned a moderate thermal inertia ($7 \times 10^{-3} \text{ cal/cm}^2\text{-sec}^{1/2}\text{-K}$). In this run (#35) the substrate **albedo** was 0.2, the frost **albedo** was 0.8, the frost emissivity was 0.6 and the global N₂ inventory was 50 kg / m². Polar caps develop, but sublime from the center out, thus developing "**polar bald spots**". The south polar cap is observed to last much longer than the north polar cap, as Pluto moves through aphelion. Two peaks in atmospheric pressure are observed per Pluto year, with the one following perihelion being more pronounced. In this particular case, the next maxima is reached just after 2000 AD, and persists to '2020. The temperature curves show that there will be times that the temperature of Pluto measured from the earth will be just the temperature of the frost deposit.

Figure 5. Sometimes transitional cap / band cases are observed, usually in the case of a cold (high **albedo** or high emissivity) frost. This configuration also occurs with a relatively large N₂ inventory. The case shown here is run #38, which had a thermal

inertia of 1×10^{-3} cal / cm²-sec^{1/2}-K, a substrate **albedo** of 0.2, a frost **albedo** of 0.8, a frost emissivity of 0.8, and a nitrogen inventory of 100 kg / m². A permanent **zonal** band forms but the frost is still mobile enough seasonally to form seasonal polar caps.

Figure 6. Run #31, shown here, is a low thermal inertia case. This run had a thermal inertia of 1×10^{-3} cal / cm²-sec^{1/2}-K, a substrate **albedo** of 0.2, a frost **albedo** of 0.8, a frost **emissivity** of 0.8, and a nitrogen inventory of 50 kg / m². Seasonal caps without polar bald spots form. The south polar cap is still observed to persist longer than the north polar cap, but differences are not as great, because the north polar cap is able to condense earlier and sublime later than in the moderate inertia case. Atmospheric pressure variation is most pronounced for these low thermal inertia cases, with orders of magnitude difference between the maxima and minima.

Figure 7. This "**dark frost**" run has the best fit set of parameters for Triton: a thermal inertia of 7×10^{-3} cal / cm²-sec^{1/2}-K, a substrate **albedo** of 0.8, a frost **albedo** of 0.2, a frost emissivity of 1.0, and a nitrogen inventory of 50 kg / m². Although Triton observable were predicted very well by this case, it does poorly for Pluto. The frost is assumed to be dark, overlying a bright substrate. Although whole disk **albedo** decreases over the last 30 years, the match of **albedo** boundaries to observable is poor. This model run would predict that one would see not only a bright south pole, but that the entire southern hemisphere would be bright. All "**dark frost**" cases predicted formation of polar caps. Two peaks in atmospheric pressure are observed.

Figure 8. This case shows a good match to **albedo** boundaries, but performs poorly in predicting disk-integrated **albedo** and atmospheric pressure. This was run #34, which had a thermal inertia of 1×10^{-3} cal / cm²-sec^{1/2}-K, a substrate **albedo** of 0.2, a frost **albedo** of 0.8, a frost emissivity of 0.6, and a nitrogen inventory of 50 kg / m².

Figure 9. This case is the best match to observable so far, although it is not perfect. This is run #12, which had a thermal inertia of 7×10^{-3} cal / cm²-sec^{1/2}-K, a substrate **albedo** of 0.2, a frost **albedo** of 0.8, a frost emissivity of 0.8, and a nitrogen inventory of 50 kg / m². The remnants of last Pluto year's south polar cap would have been visible in 1955, but this run does not predict formation of the new cap in time for the 1985-88 observations of a bright south pole. It does predict dark south mid-latitudes and bright north mid-latitudes, but unfortunately also predicts a bright north polar cap. (Earlier formation of a north polar bald spot would solve this **problem!**) Whole disk **albedo** would have decreased from 1955 to 1970, but a recent upturn should have been observed. Atmospheric pressure was in the right ballpark in 1988, and will reach its peak in " 2005. The peak will persist until '2025.

Modelling the Pluto-Triton Pair (cont.)

Characteristic	Triton	Pluto	Model Significance
Radius (km)	1350	1150	
Density (kg/m ³)	2080	2129	Assume similar rock content → similar internal heat flow
Surface gravity (m/sec ²)	0.79	0.68	
Sidereal period (yrs)	163.7	248.0	Somewhat similar seasonal thermal wave depth
Rotational period (days)	5.58	6.39	Very similar diurnal thermal wave depth
Volatiles detected on surface or in atmosphere	N ₂ , CH ₄ , CO, CO ₂	N ₂ , CH ₄	Assume N ₂ is dominant volatile
Atmospheric Pressure (Pa) (assuming vapor pressure equilibrium)	1.6	0.126 (N ₂) 0.049 (CH ₄)	Model should predict for 1989
Albedo, equator / pole	0.6/0.9	0.4/0.9	

Table 1

Table 2. Thermal Model Runs

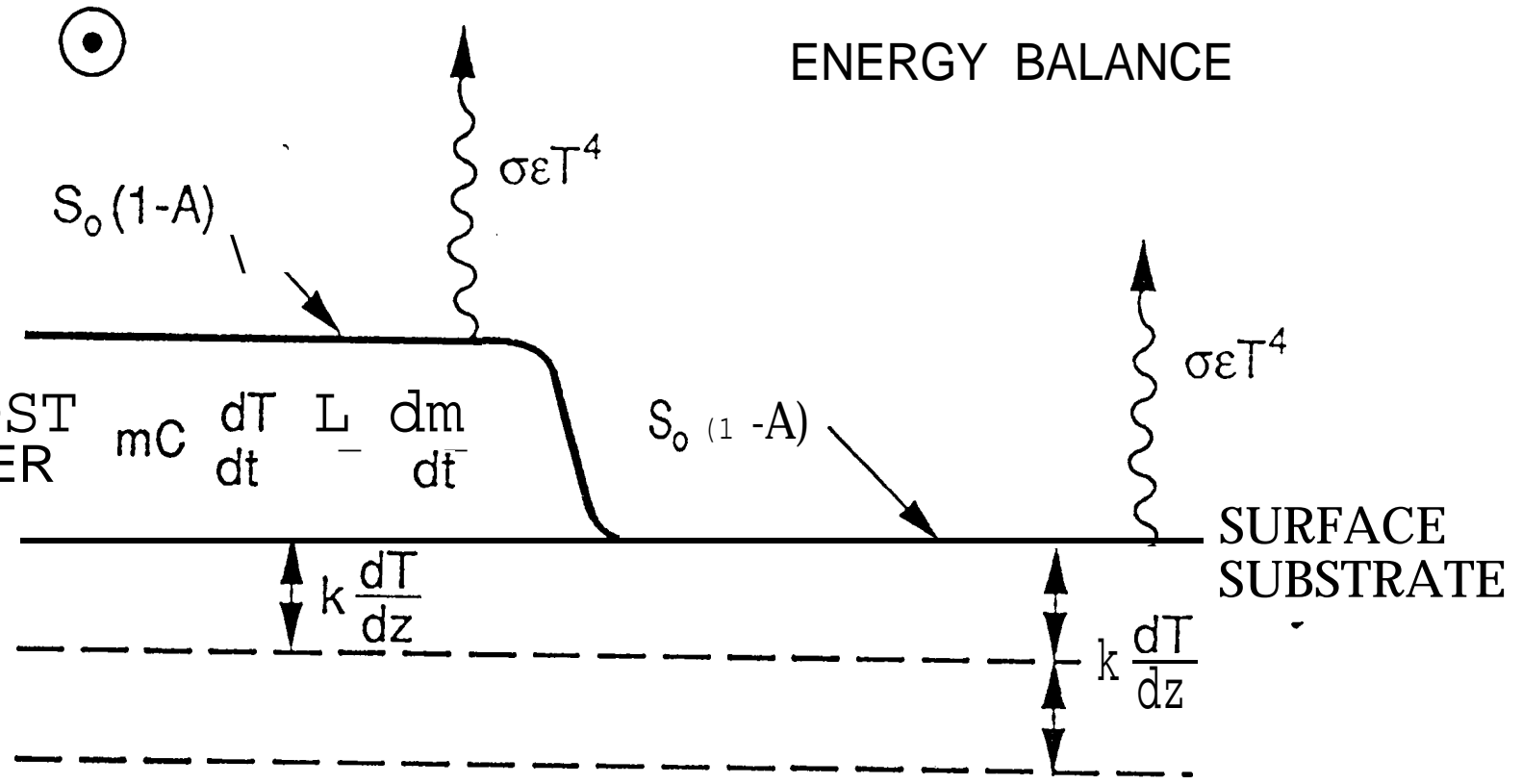
Run #	Thermal Inertia x 10 ⁻³	Substrate Albedo	Frost Albedo	Frost Emissivity	N2 Inven- tory
-----	-----	-----	-----	-----	-----
1	7	0.8	0.2	1.0	50
2	7	0.8	0.2	1.0	100
3	7	0.8	0.2	1.0	200
4	1	0.8	0.2	1.0	50
5	50	0.8	0.2	1.0	50
11	7	0.4	0.8	0.6	50
16	1	0.4	0.8	0.6	50
17	7	0.4	0.8	0.8	50
18	1	0.4	0.8	1.0	50
13	1	0.3	0.9	0.8	50
31	1	0.2	0.8	0.8	50
33	1	0.2	0.8	1.0	50
34	1	0.2	0.8	0.6	50
37	1	0.2	0.8	0.6	100
38	1	0.2	0.8	0.8	100
41	1	0.2	0.8	0.8	200
12	7	0.2	0.8	0.8	50
15	7	0.2	0.8	0.8	100
35	7	0.2	0.8	0.6	50
30	7	0.2	0.8	1.0	50
40	7	0.2	0.8	0.8	200
43	7	0.2	0.8	0.6	100
14	50	0.2	0.8	0.8	50
32	50	0.2	0.8	1.0	50
36	50	0.2	0.8	0.6	50

Table 3. Depths of the Diurnal and Seasonal Thermal Waves for Different Thermal Inertias of the Substrate

Thermal Inertia X 10 ⁻³ cal / cm ² -sec ^{1/2} -K -----	Diurnal thermal wave depth (m) -----	Seasonal thermal wave depth (m) -----
1	0.02	2.1
7	0.12	15
50	0.88	105

Primary input variables:

- Surface albedo
- Surface emissivity
- Surface albedo
- Surface thermal inertia
- Ice inventory



FROST LAYER $mC \frac{dT}{dt} - L \frac{dm}{dt}$

$S_0(1-A)$

$\sigma\epsilon T^4$

$k \frac{dT}{dz}$

$k \frac{dT}{dz}$

$$C_p \frac{dT}{dt} = S_0(1-A) - \epsilon\sigma T^4 + L \frac{dm}{dt} + k \frac{dT}{dz} + L_{up} \frac{dm_{up}}{dt}$$

Fig. 2 Pluto's Seasons

This portion of orbit characterized by rapid crossing of subsolar pt from $\sim 60^\circ$ south to equator to $\sim 60^\circ$ north

Expect slow condensation of north polar cap in this quadrant

High eccentricity orbit

South pole \sim facing sun

Perihelion: fastest motion

Aphelion: slowest motion

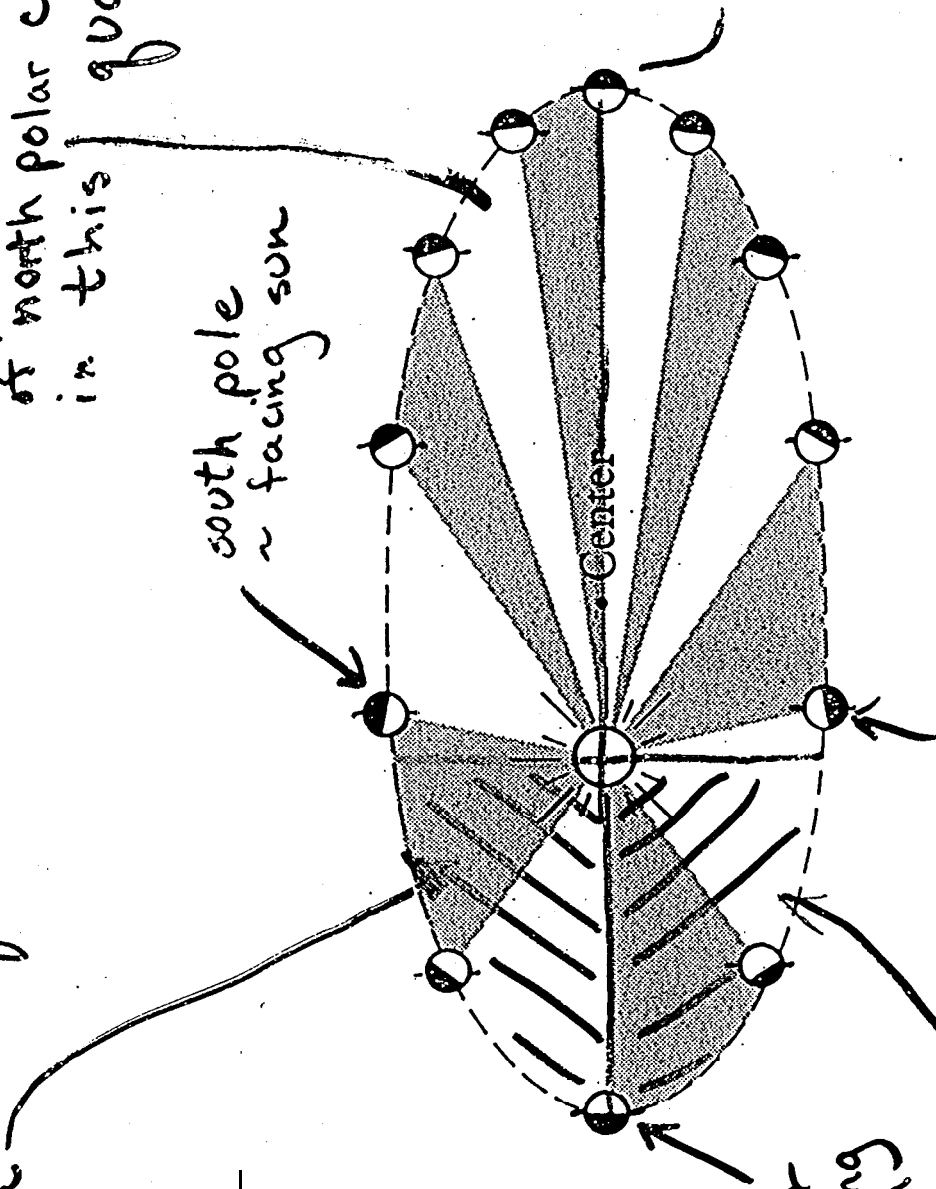
equator facing sun

equator facing sun

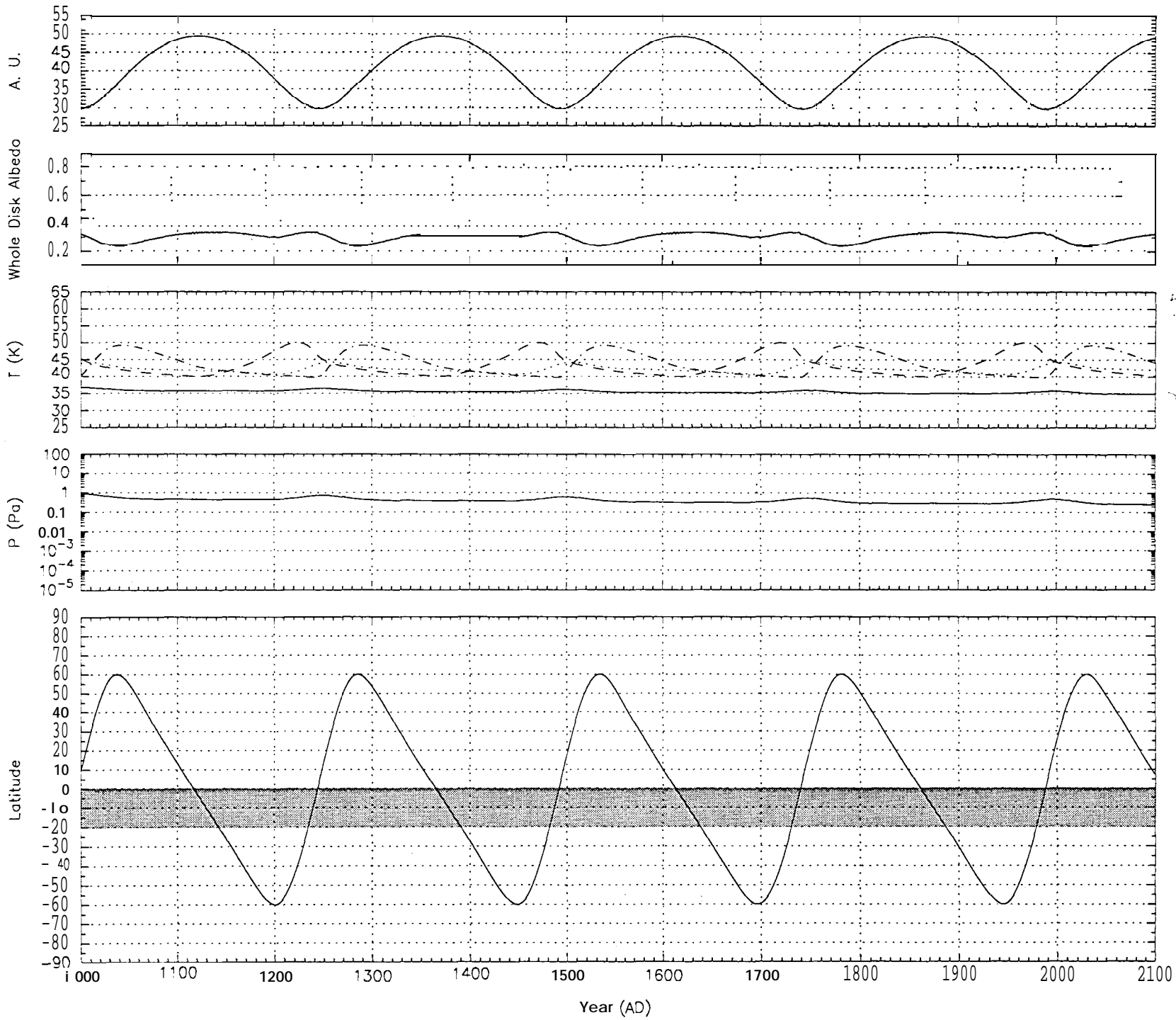
North pole \sim facing sun

Expect rapid condensation of south polar cap in this quadrant, relatively more rapid sublimation of north cap than south

Pluto's obliquity $\sim 120^\circ$
 Annual insolation at poles $>$ annual insolation at equator



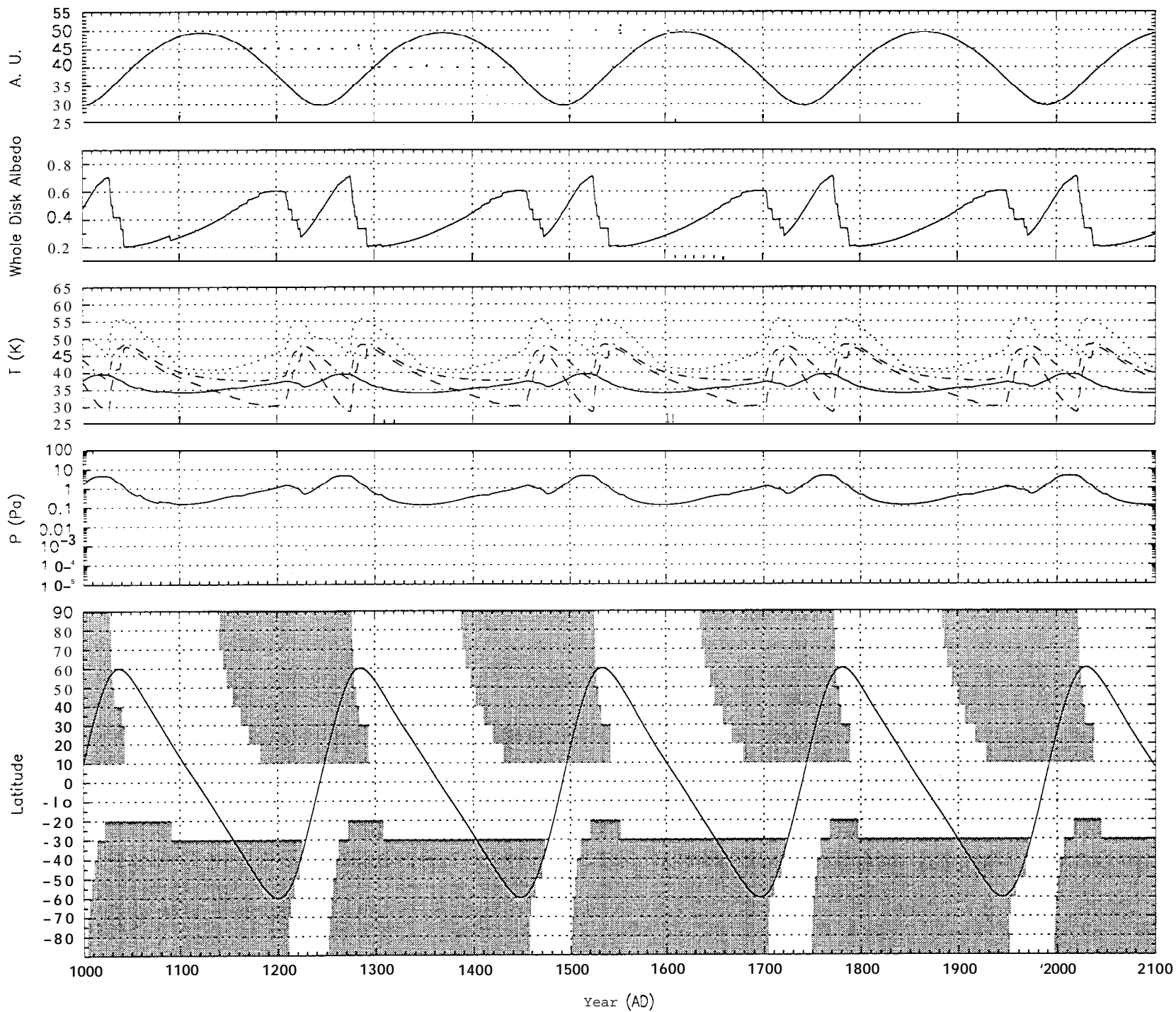
run32



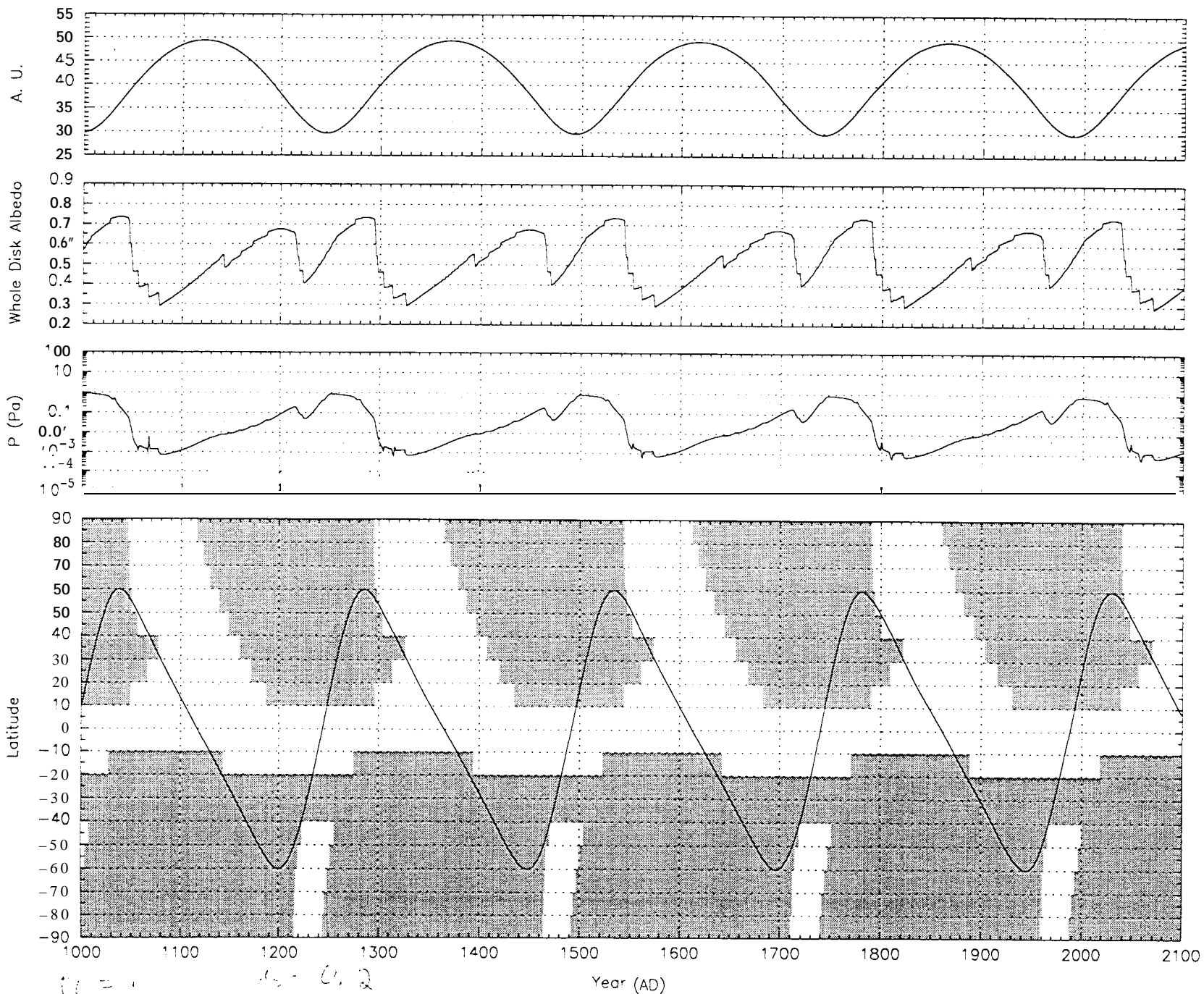
Handwritten notes:
+10 1st
+10 2nd
+10 3rd

Handwritten mark: a small scribble or signature.

otme35

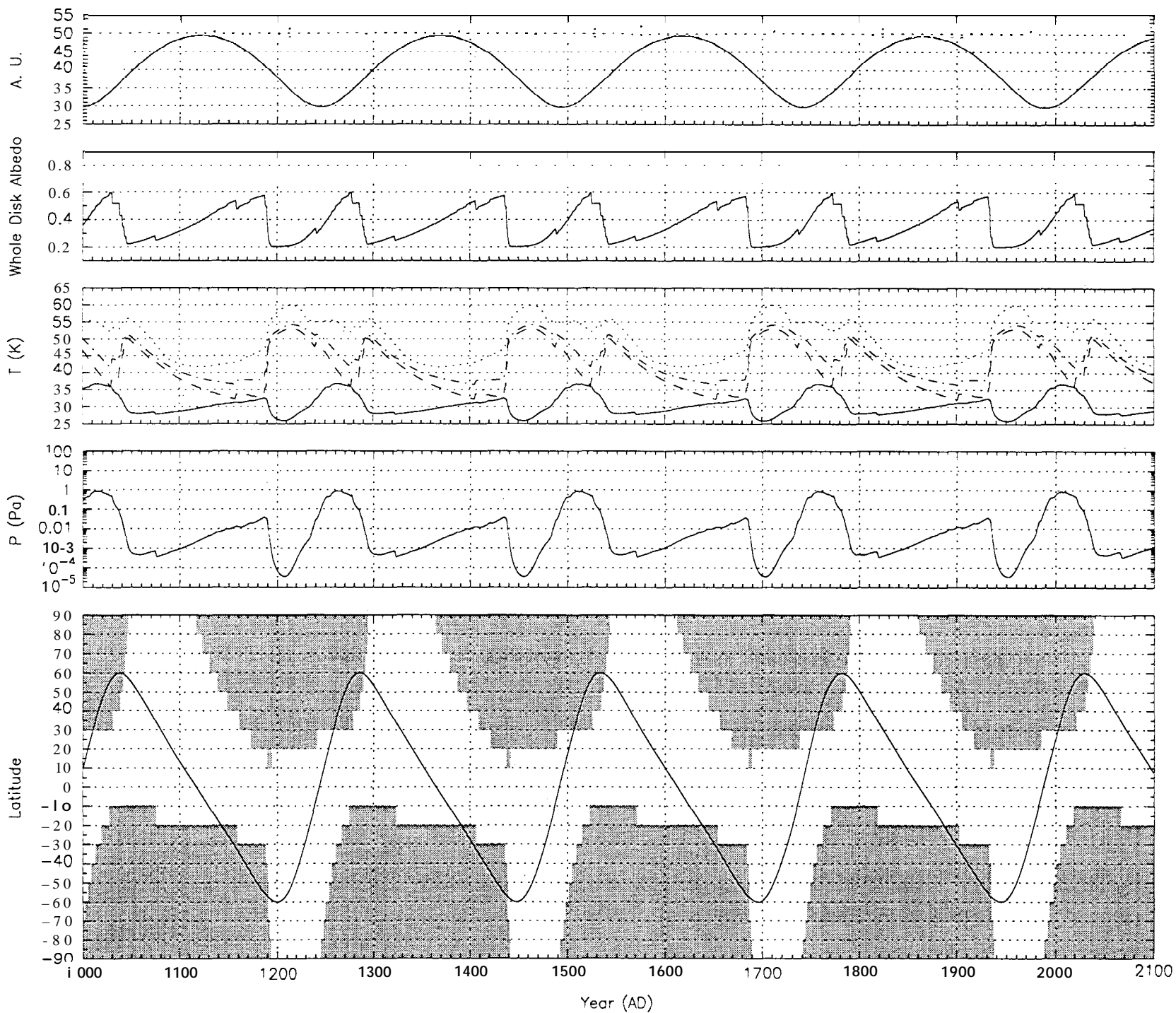


otime38



$\epsilon = 1$
 $\epsilon = 0.2$
 $\delta = 100$
 $\delta = 0.8$
 $\delta = 0.8$

otme31



ptme1

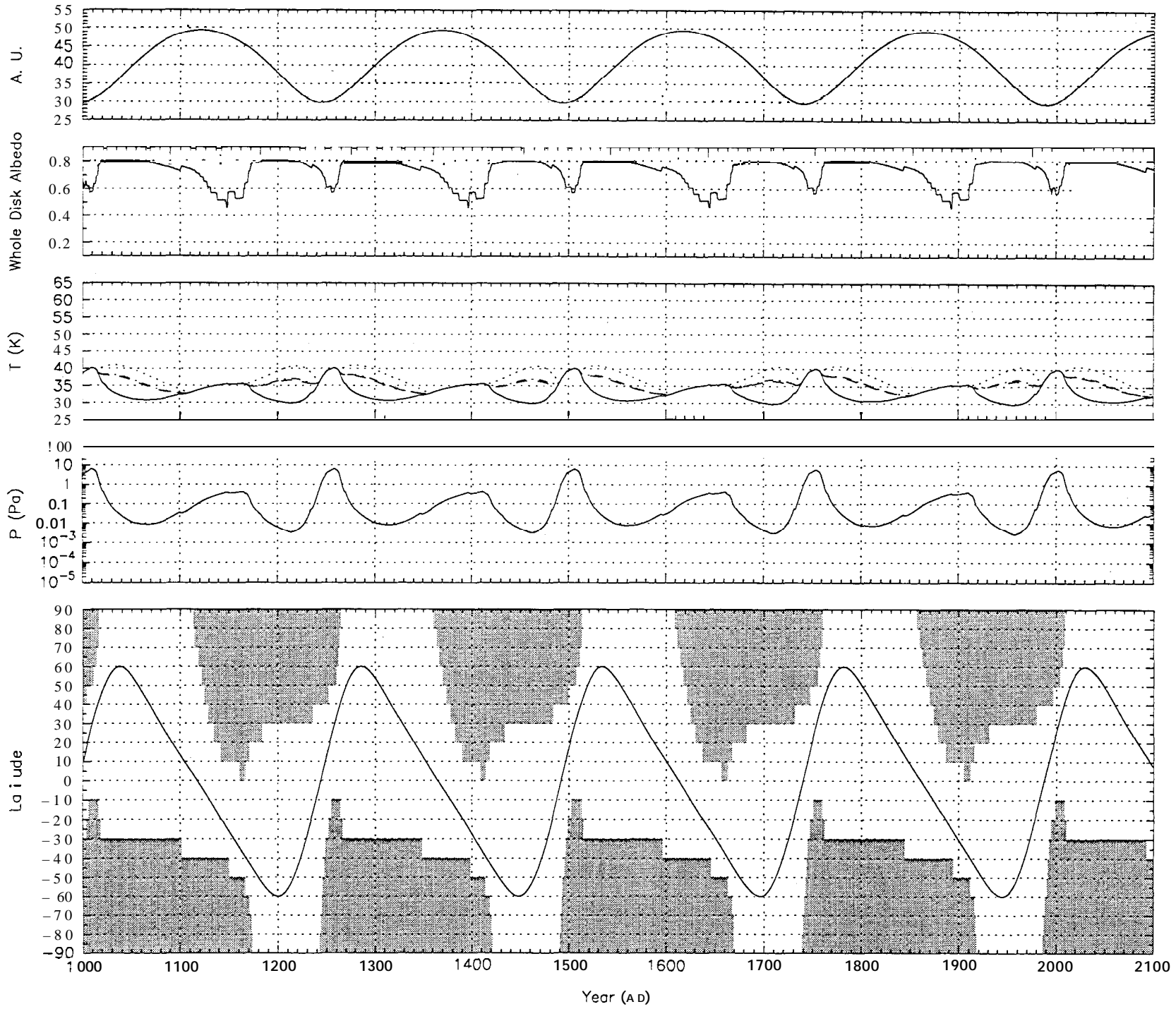
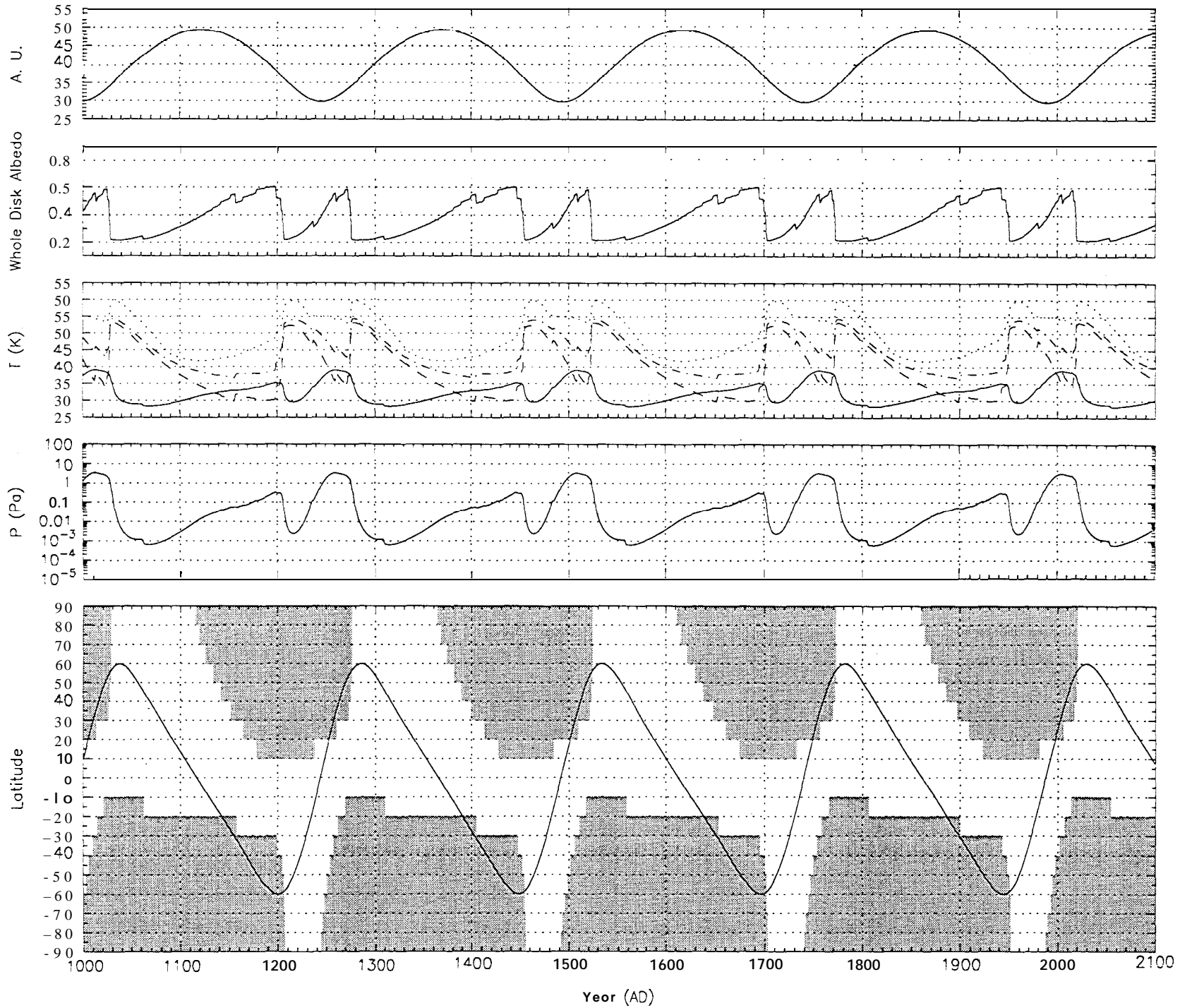


Fig 4

dtme34



T r

ptme12

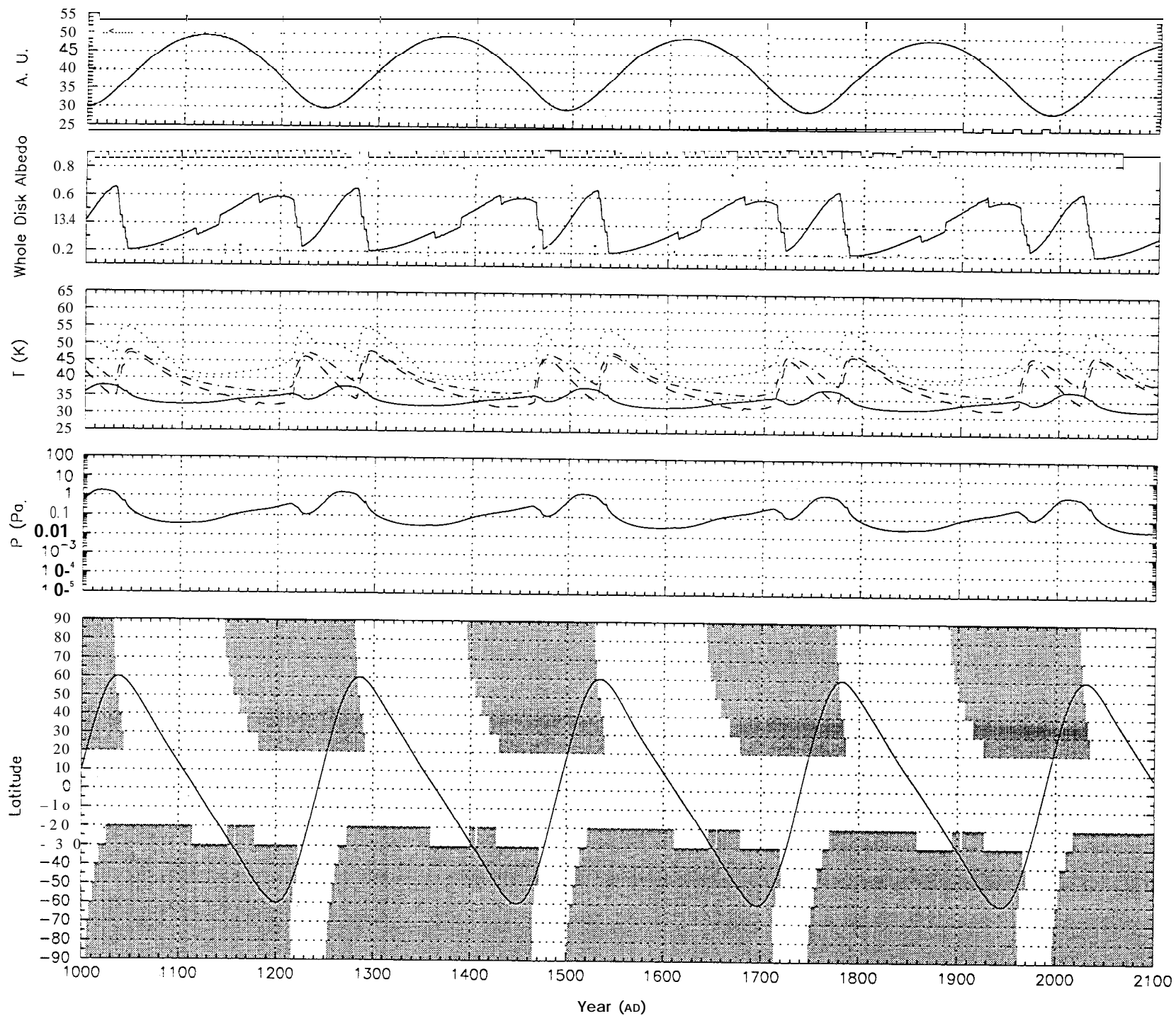


Fig. 11